

## Cooling-assisted cold-pressing: a sustainable approach to high-quality hemp seed oil extraction

Maura Sannino <sup>a,1</sup>, Simona Piccolella <sup>b,1</sup>, Guglielmo Maresca <sup>a</sup>, Francesco Siano <sup>c</sup>, Gianluca Picariello <sup>c</sup>, Severina Pacifico <sup>b,\*</sup>, Salvatore Faugno <sup>a</sup>

<sup>a</sup> Department of Agricultural Sciences, University of Napoli Federico II, 80055 Portici (NA), Italy

<sup>b</sup> Department of Environmental, Biological & Pharmaceutical Sciences and Technologies, University of Campania 'Luigi Vanvitelli', Via Vivaldi 43, 81100 Caserta, Italy

<sup>c</sup> Istituto di Scienze dell'Alimentazione - CNR, Avellino, Italy

### ARTICLE INFO

#### Keywords:

Hemp seed oil  
Cold-pressing  
Cooling system  
Oil quality  
ATR FT IR spectroscopic analysis  
UHPLC HR MS analysis

### ABSTRACT

Hemp seed oil (HSO) is valued for its rich nutritional profile and bioactive compounds, including polyunsaturated fatty acids, tocopherols, and phytosterols. As demand for sustainable, high-quality functional foods grows, optimizing extraction methods is essential to preserving these compounds while ensuring environmental responsibility. Mechanical cold pressing is a preferred method because it avoids the use of chemical solvents; however, excessive mechanical friction can increase temperatures, leading to oxidation and nutrient degradation. This study evaluates the effect of an integrated cooling system (CO) versus a non-cooled system (NCO) in HSO extraction. A screw press with a copper coil cooling mechanism and food-grade propylene glycol coolant was designed to regulate temperatures, monitored via thermal imaging and resistance temperature detectors. Key oil quality parameters, including peroxide value, free acidity, fatty acid profile, tocopherol, phenolic content, and phytosterol composition, were analyzed. Results show that the CO system reduced extraction temperatures (by 11 % in the compression chamber and 15 % in the extracted oil), enhancing oxidative stability and bioactive retention, particularly phenolics, while maintaining oil yield and efficiency. Integrating cooling technologies into industrial cold pressing offers a sustainable solution to enhance nutritional stability, extend shelf life, and reduce oxidative waste, aligning with the shift toward eco-friendly food processing.

### 1. Introduction

Oilseeds play an increasingly important role in both human and animal nutrition, as sources of edible oil and also for their bioactive components with potential therapeutic effects. Recent studies have shown, for example, that watermelon seed-fortified crackers can help reduce hyperlipidemia in rats (AlMasoud et al., 2024), and that seed extracts from *Opuntia ficus-indica*, *Azadirachta indica*, and *Lepidium sativum* exhibit antidiabetic and hepatoprotective properties in animal models (Saleh et al., 2023; Hafeez et al., 2024). Among oilseeds, hemp seed (*Cannabis sativa* L.) is gaining increasing attention due to its balanced nutritional composition and versatile applications. In addition to being a valuable source of plant protein and dietary fiber, hemp seed contains a significant proportion of lipids, making it suitable for oil extraction. In particular, hemp seed oil (HSO) is increasingly recognized as a sustainable and nutritionally valuable ingredient in the future foods

industry. It is a rich source of polyunsaturated fatty acids (PUFAs), phytosterols, tocopherols (UNI 11876:2022), and other bioactive compounds, which contribute to its antioxidant, anti-inflammatory, and cardiovascular benefits (Crescente et al., 2018). Owing to these properties, hemp seed and its oil have been incorporated into a range of innovative food applications, including plant-based dairy alternatives, protein-enriched bars, salad dressings, and nutritional supplements, underlining its versatility in the development of functional foods (Montero et al., 2023). Furthermore, its suitability for clean-label, allergen-free, and vegan formulations reinforces its relevance in the design of sustainable and health-promoting dietary solutions (Mistry et al., 2025). In this context, the growing consumer demand for minimally processed, plant-based, and environmentally responsible products underscores the need to optimize extraction techniques, with the aim of preserving nutritional quality while reducing environmental impact.

Among available extraction techniques, cold pressing is widely

\* Corresponding author.

E-mail address: [severina.pacifico@unicampania.it](mailto:severina.pacifico@unicampania.it) (S. Pacifico).

<sup>1</sup> These authors equally contributed

considered the most sustainable method, as it avoids the use of chemical solvents and reduces energy consumption compared to other industrial extraction processes (Izzo et al., 2020; Tura et al., 2023). However, the efficiency of cold pressing is influenced by several factors, particularly the size of the nozzle in the pressing system (Faugno et al., 2019). While smaller nozzles increase internal pressure and enhance friction, facilitating oil release, they also raise extraction temperatures, which can have both positive and negative effects. Moderate heat improves oil flow and efficiency, but excessive temperatures accelerate oxidation and degrade heat-sensitive compounds such as tocopherols and essential fatty acids (Ionescu et al., 2014; Kraljić et al., 2013).

Despite being classified as a cold extraction method, mechanical friction can cause localized temperature spikes exceeding 70 °C, depending on pressing conditions. Studies indicate that temperatures above 50–60 °C can compromise oil quality, leading to oxidation, hydrolysis, and degradation of key bioactive compounds (Senphan et al., 2025; Muangrat and Kaikongjanat, 2025). Another often overlooked yet critical sustainability factor is the initial moisture content of the seeds (Senphan et al., 2025). Improper post-harvest drying can increase free fatty acid levels, leading to rancidity, and amplify energy consumption during processing due to excessive heat generation. High moisture content in seeds can also create emulsions that reduce extraction efficiency, resulting in resource waste. Additionally, moisture retention in improperly stored seeds increases the risk of microbial growth and mycotoxin contamination, further compromising oil safety and sustainability.

Beyond compositional changes, high extraction temperatures also affect sensory properties, leading to undesirable alterations in flavor, aroma, and color. Heat exposure can degrade chlorophyll and carotenoids, shifting the oil color from vibrant green to yellowish tones, a common sign of oxidative deterioration (Siano et al., 2019). Temperatures above 70 °C can accelerate deterioration processes, including lipid oxidation and thermal degradation, beyond the effects of enzymatic lipolysis, increasing free acidity, a key indicator of oil degradation and reduced shelf life. Therefore, ensuring thermal control during pressing is essential to preserve the oil nutritional quality, reduce waste and support sustainability in food systems (Piravi-Vanak et al., 2024; Senphan et al., 2025).

To address these challenges, this study conducted a comparative analysis of two cold-pressing methods: one with an integrated cooling system (CO) and one without cooling (NCO), using the same seed batch to eliminate variability due to raw material differences. The primary objective was to assess whether active temperature control during extraction could enhance oil stability and reduce oxidative degradation, contributing to a more efficient and sustainable production process. Key nutritional and oxidative stability markers were monitored monthly for six months, focusing on fatty acid composition (PUFA, ω-3, ω-6), phytosterol content, total phenolic content, photosynthetic pigments (chlorophylls, carotenoids), and cannabidiolic acid.

In addition to freshly extracted oil, the study also investigated the bioactive compound content in the precipitate formed after natural sedimentation (decantation process). This fraction is often discarded, yet it may contain valuable secondary metabolites that could contribute to the oil functional properties. Exploring ways to recover and utilize these bioactive-rich fractions aligns with the principles of circular economy and zero-waste food processing. By systematically evaluating the interactions between seed moisture, extraction temperature, and bioactive compound retention, this research provides a comprehensive strategy for refining cold-pressing protocols. Optimizing these parameters ensures high oil yield, extended shelf life, and superior nutritional stability, while reducing energy consumption, waste, and resource inefficiencies. Given the increasing demand for high-quality, bioactive-rich, and eco-conscious oils, improving extraction technologies represents a crucial step toward a more sustainable and resilient food system.

## 2. Materials and methods

### 2.1. Hemp seed oil cold pressing procedure

In the experimental study hemp seeds were harvested from an experimental field in Sicily (Italy). The selected variety, "Futura 75" ( $\Delta^9\text{-THC} \leq 0.2\%$ ), is registered in the EU Common Catalogue and valued for its adaptability to Mediterranean conditions (Calzolari et al., 2021). It yields approximately 22–30 % oil, depending on harvest time, and features a favourable fatty acid profile, rich in linoleic and  $\alpha$ -linolenic acids. Tests were performed in the engineering laboratory at the Agriculture Department of the University Federico II of Naples (Italy). Seeds were preliminarily cleaned to separate impurities with a pneumatic cleaner, then dried in a crossflow dryer providing an air stream at 40 °C temperature and equipped with a screw to distribute the airflow uniformly over the seeds. Subsequently, seeds were sorted with a sieving machine consisting of four oscillating sieves that removed hollow seeds, coarse dust and small stones. Finally, the seeds were stored in sealed jars at a temperature between 15 and 25 °C, provided that the moisture content, determined in an air oven (BD115, BINDER GmbH, Tuttlingen, Germany) set at  $105 \pm 1$  °C, was low enough (8 % w/w) to prevent microbial spoilage. In both the CO and NCO trials, seven replicant extractions were executed with 1 Kg of seeds. Seeds were pressed with a Bracco screw press (Bracco s.r.l., Bagnatica, Bergamo, Italy) powered by a 2.2 kW electric motor and mounting a heat exchanger to keep the extraction temperature constant in the press chamber (Fig. 1). The equipped nozzle diameter was 8 mm, based on the evidence that small nozzles enhance oil yield at high extraction temperatures (Faugno et al., 2019; Karaj and Müller, 2011; Sannino et al., 2024). The cooling system consisted of a copper coil wrapping longitudinally the external surface of the compression chamber. The coolant consisted of food-grade propylene glycol diluted 40 % with distilled water. A pump connected to the coil provided a continuous flow of liquid chiller into the circuit. The length of the coil, the temperature of the coolant and the speed of the pump were set to achieve an extraction temperature of 70 °C within the compression chamber since this value allowed higher oil yields in previous research (Faugno et al., 2019). Based on the same research, the screw speed was set at 22 rpm. Extracted oil samples were individually stored in lightproof plastic containers. Raw oil was refined by centrifugation to remove impurities like FFAs, waxes and gums through an ALC centrifuge (ALC T535 PK130R, Winchester, United States) at 3500 rpm for 20 min.

The extraction temperature was monitored in two stages. The first detection occurred in the compression zone by a resistance temperature detector (RTD) type Pt100, while the second was set at the extracted oil after the release from the compression cylinder. Furthermore, an infrared thermal camera (model FLIR E54, Teledyne FLIR LLCM, Wilsonville, Oregon) was installed to produce detailed representations of the thermic variations throughout the extraction process. The camera was installed on a tripod and, 5 different photos of each replicate were taken during the extraction. Technical features of the camera are: 25° fixed-lens, temperature detection range between –20 °C and +120 °C, thermal sensibility of 50 mK, IRT resolution of 0,01 °C, with an accuracy of 2 % over a given range. Calibration to environment temperature was performed using a grey body before each measurement session. The thermograms were saved on a memory card and then analysed with the software FLIR Tools, considering an emissivity of 0.98 to calculate the mean temperatures in a given region. To obtain a comprehensive overview of the extraction dynamics, five point-shaped markers (P1-P5), one linear marker obtained ("LINE", corresponding to the longitudinal section of the press) and one aerial marker ("AREA") were selected for quantitative analysis of the temperature. The screwing speed was measured by a variable speed controlled connected to a tachometer. All data were collected using a compact-DAQ chassis (Model cDAQ-9171, National Instruments, Austin, TX, United States) and then transferred for processing using LabView software.

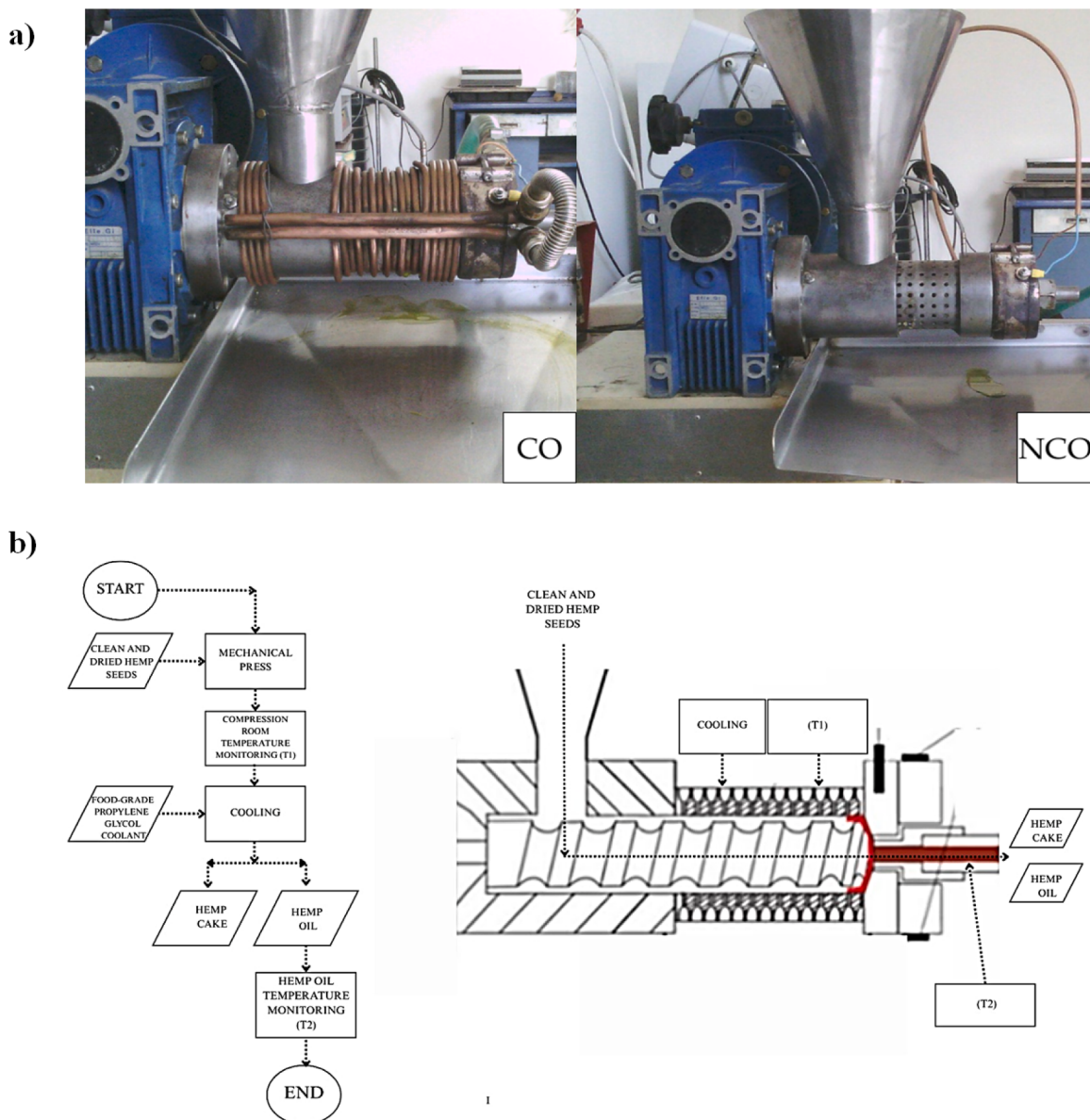


**Fig. 1.** a) Screw press machine equipped with the cooling system (CO) and without it (NCO); b) b) flowchart realized according to ISO 5807:1985 and cross-sectional diagram of cold-press hemp seed oil extraction showing temperature monitoring (T1, T2) and cooling system using food-grade propylene glycol.

During the trials, the measured variables were the compression zone temperature ( $T_1$ , °C); extracted oil temperature ( $T_2$ , °C); oil gross weight (OGW, g); oil cake gross weight (CGW, g); extraction time ( $t$ , mm: ss). The work rate of the cold press (PWR) was assessed as reported by (Crimaldi et al., 2017), by dividing the seed weight (SW) by  $t$ , while the oil yield ( $y$ , % w/w) was obtained by dividing the SW by OGW. The energy consumption (ES, in kWh kg<sup>-1</sup> of processed seeds) was calculated by dividing the total energy (TE, in kWh) by the sample size (S, in kg). The average power (P, in kW) was multiplied by the average pressing time ( $t$ , in h) required for each sample to calculate TE.

## 2.2. Oil quality parameters

### 2.2.1. Free acidity determination

A 2.5 g aliquot of each HSO sample was dissolved in 25 mL of a mixture containing diethyl ether/ethanol (1:1, v/v), and titrated with KOH 0.1 N, using phenolphthalein (0.1 % solution in ethanol) as the indicator.

The results were expressed as free acidity, i.e. the percentage of oleic

acid (OA %) (Eq. (1)).

$$OA (\%) = \frac{0.0282 \times V}{m} \times 100 \quad (1)$$

where  $V$  = mL KOH used for titration,  $m$  = g of the HSO sample (CODEX STAN 210-1999). Six replicates for each sample were performed and the results were expressed as mean values  $\pm$  standard deviation (SD).

### 2.2.2. Peroxide value assessment

The peroxide value was assessed through an iodometric titration. Briefly, a 5 g aliquot of each hemp seed oil sample was placed in a CH<sub>3</sub>COOH:CHCl<sub>3</sub> solution (3:2, v/v), and 0.5 mL of KI-saturated aqueous solution was added. After shaking for 1 min, the flask was maintained in the dark for 5 min. Then, distilled water (75 mL) was added, and the titration was performed with a Na<sub>2</sub>S<sub>2</sub>O<sub>3</sub> solution (0.01 N), using a 1 % starch solution as the indicator.

The peroxide number (PV), expressed as meq of O<sub>2</sub> per kg of oil, was calculated as follows (Eq. (2)):

$$PV = \frac{V \times N}{m} \times 1000 \quad (2)$$

where  $V$  = mL of  $\text{Na}_2\text{S}_2\text{O}_3$  used for titration,  $N$  = normality of the  $\text{Na}_2\text{S}_2\text{O}_3$  solution,  $m$  = g of the HSO sample (CODEX 2011). The measurement was repeated after 30 and 60 days to monitor the oil oxidative stability over time. Six replicates for each sample were performed and the results were expressed as mean values  $\pm$  SD.

### 2.2.3. Spectrophotometric investigation in the UV region

Aliquots of each HSO sample were dissolved in isoctane ( $10 \text{ mg mL}^{-1}$ ) under continuous stirring. The absorbance of the obtained solutions was recorded at 232, 264, 268, and 272 nm in reference to a blank by a Cary 100 instrument (Agilent, Milano, Italy). Extinction coefficient  $K$  (the extinction of 1 % solution of the fat in the specified solvent, at a thickness of 1 cm) at the considered wavelengths was determined, as well as  $\Delta K$ , as follows (Eq. (3)):

$$\Delta K = Km \frac{(K_{\lambda m} - 4) + (K_{\lambda m} + 4)}{2} \quad (3)$$

where  $K_{\lambda m}$  is the specific extinction at the maximum absorption wavelength of 268 nm in isoctane (COMMISSION REGULATION (EU), 2006). Three replicates for each sample were performed and the results were expressed as mean values  $\pm$  SD.

### 2.2.4. Free fatty acid and CBDA profiling

Aliquots of each HSO sample were diluted in *n*-hexane (1:15, v/v), filtered on 0.2  $\mu\text{m}$  RC membrane syringe filters (Millex, Phenomenex, Torrance, CA, USA), and 2  $\mu\text{L}$  of the solutions immediately underwent UHPLC–HRMS analysis. To this purpose, the NEXERA UHPLC system (Shimadzu, Tokyo, Japan) was employed, equipped with a Luna® Omega C18 column (50 mm  $\times$  2.1 mm i.d., 1.6  $\mu\text{m}$  particle size; Phenomenex, Torrance, CA, USA). The chromatographic method consisted of a linear gradient of water (W) and acetonitrile, both acidified with 0.1 % formic acid, at a flow rate of 0.5  $\text{mL min}^{-1}$ , as follows: 0–0.5 min, 45 % W; 0.5–7.5 min, 45 %  $\rightarrow$  10 % W; 7.7–8.5 min, 10 % W. Then, the initial conditions were restored and kept for 1.5 min. The UHPLC was coupled with the AB SCIEX TripleTOF® 4600 mass spectrometer (AB Sciex, Concord, ON, Canada), equipped with a DuoSpray™ ion source operating in negative electrospray (ESI) ion mode, while the APCI probe was used for automated mass calibration in all scan functions using the Calibrant Delivery System (CDS). The untargeted HRMS analysis consisted of a full scan TOF survey in the mass range 150–500 Da with an accumulation time of 250 ms and eight Information-Dependent Acquisition (IDA) MS/MS scans in the mass range 80–450 Da with an accumulation time of 100 ms. The source parameters in the TOF-MS experiments were optimized and set as follows: curtain gas 35 psi, nebulizer and heated gases 60 psi, ion spray voltage  $-4.5 \text{ kV}$ , interface heater temperature  $600^\circ\text{C}$ , declustering potential 60 V. TOF-MS/MS analyses were performed at a collision energy of 45 V with a spread of 25 V. The instrument was controlled by the Analyst® TF 1.7 software, while data processing was carried out using the PeakView® software version 2.2.

The quantitative determination of cannabidiolic acid (CBDA) was achieved on a Kinetex® PS C18 column (50 mm  $\times$  2.1 mm i.d., 2.6  $\mu\text{m}$  particle size; Phenomenex, Torrance, CA, USA), using the HPLC 1260 INFINITY II (Agilent Technologies, Santa Clara, CA, USA), equipped with an Agilent G7129A autosampler, an Agilent GY115A DAD-UV-visible detector (set at  $266 \pm 4$  and  $306 \pm 4$  nm) and a Quaternary pump Agilent G711A.

### 2.2.5. Chlorophyll and carotenoid content

Aliquots of 100 mg of HSO samples were diluted with diethyl ether up to a volume of 3 mL, vortexed, and sonicated for 1 min (Ultrasonics™ Bransonic™ M3800-E; Danbury, CT, USA). Then, UV-Vis spectra were recorded by a Cary 100 instrument (Agilent, Milano, Italy) in reference

to a blank and the chlorophyll and carotenoid content was calculated as previously reported (Izzo et al., 2020). Three replicates for each sample were performed and the results were expressed as mean values  $\pm$  SD.

### 2.2.6. Extraction and quantification of tocopherols

Aliquots of each HSO sample (10 g) were diluted in EtOH (8 mL), and pyrogallol (100 mg) and KOH (60 % w/w, 4 mL) were added, purging the solution under a  $\text{N}_2$  flow. After stirring for 10 min in the dark, water (50 mL) was added to the flask, and the mixture was transferred into a separating funnel and extracted with diethyl ether (50 mL). The upper phase was recovered, and the water phase was extracted four times with diethyl ether (30 mL each). The pooled organic phases were sequentially washed with water (50 mL), and HCl 0.01 M. Anhydrous sodium sulfate was used to remove any water traces from the ether phase. Finally, the samples were filtered and the solvent evaporated under vacuum. Aliquots of each obtained sample were diluted in acetonitrile (1:30, v/v), filtered on 0.2  $\mu\text{m}$  RC membrane syringe filters (Millex, Phenomenex, Torrance, CA, USA), and 2  $\mu\text{L}$  of the solutions underwent HPLC-UV analysis for  $\alpha$ -,  $\beta$ -,  $\gamma$ -, and  $\delta$ -tocopherol quantitation. To this aim, the HPLC 1260 Infinity II (Agilent, Santa Clara, CA, USA), equipped with an Agilent G711A quaternary pump and a WR G7115A diode array detector, was used. The chromatographic separation was optimized on a Kinetex® Biphenyl column (50  $\times$  2.1 mm i.d., 2.6  $\mu\text{m}$  particle size, Phenomenex, Torrance, CA, USA) eluting with MeOH/water (85:15, v/v), both acidified with formic acid (0.1 %) in isocratic conditions at  $35^\circ\text{C}$  oven temperature and a flow rate of  $0.3 \text{ mL min}^{-1}$ . The UV detection was set at 292 nm, based on the wavelength of maximum absorption of  $\alpha$ -tocopherol. Authentic  $\alpha$ -tocopherol, at varying concentrations (calibration curve in the range  $0.1$ – $200 \mu\text{g mL}^{-1}$ ) was used as the external standard for quantitation. Three replicates for each sample were performed and the results were expressed as mean values  $\pm$  SD.

### 2.2.7. Phenol extraction and total phenol content (TPC) value determination

Hemp seed oils (5 g) were diluted with *n*-hexane (1:1, w/v) and underwent liquid/liquid extraction using a MeOH:H<sub>2</sub>O solution (4:1, v/v; 10 mL), as previously described (Faugno et al., 2019).

The resulting polar fractions (CO\_PhF and NCO\_PhF; yield equal to 0.07 and 0.11 %) were tested by the Folin–Ciocalteu method, to assess their total phenolic content (TPC). Briefly, each sample was mixed with 2.25 mL of  $\text{Na}_2\text{CO}_3$  (7.5 % w/v) and 0.250 mL of the Folin–Ciocalteu reagent (FCR). After stirring the reaction mixture at room temperature for 90 min, 250  $\mu\text{L}$  of each sample were transferred into a multiwell plate and the absorbance was read at 765 nm using a Mobi® UV/Vis Microplate Spectrophotometer (MicroDigital Co., Ltd., Seongnam, Republic of Korea). The results were expressed as milligrams of gallic acid equivalents (GAE) per gram of the sample. Three replicates for each sample were performed and the results were expressed as mean values  $\pm$  SD.

### 2.2.8. Extraction and quantification of phytosterols

The sample preparation for phytosterol analysis was performed as described by Aloisi et al. (2020) with slight modifications. Briefly, the internal standard ( $\alpha$ -cholestane, 2  $\text{mg mL}^{-1}$ , 0.5 mL) and 25 mL of a 2 N KOH ethanolic solution were added to 2.5 g of each hemp seed oil, then heated under reflux and magnetic stirring. The complete saponification took about 20 min after solution clarification. Then, water (25 mL) was added and the solution was quantitatively transferred into a separating funnel, where three extraction steps were performed with diethyl ether (40 mL at first, and then 30–35 mL twice). The ether phases were pooled and washed with water several times (50 mL each), until neutralization (checked by the phenolphthalein indicator), and finally anhydriified with anhydrous sodium sulfate. After filtration, the solvent was evaporated under vacuum at  $30^\circ\text{C}$ . Acetone (2.5 mL) was added to the dried samples and evaporated under nitrogen flow. The solid residue was maintained in the oven at  $103 \pm 2^\circ\text{C}$  for 15 min, cooled in a desiccator, and weighed.

The samples were analyzed by gas chromatography - flame ionization detector (GC-FID) analysis, as previously described (Siano et al., 2019). A Trace GC gas chromatograph (Thermo Scientific, Inc., San Jose, CA, USA) equipped with a Flame Ionization Detector (FID) and an RTX-5 capillary column ( $30\text{ m} \times 0.25\text{ mm} \times 0.25\text{ }\mu\text{m}$ ; Restek, USA) was used. Samples ( $1\text{ }\mu\text{L}$ ) were injected in split mode (1:10 ratio) via an auto-sampler at  $250\text{ }^\circ\text{C}$ . The oven temperature program began at  $200\text{ }^\circ\text{C}$  (held for 2 min) and then increased linearly to  $300\text{ }^\circ\text{C}$  at  $20\text{ }^\circ\text{C}/\text{min}$ . Data acquisition and processing were carried out with ChromQuest 5.0 software (Thermo Scientific). Three replicates for each sample were performed and the results were expressed as mean values  $\pm$  SD.

### 2.3. Preliminary spectroscopic characterization of the solid residues after oil decantation

Aliquots of the solid residues (hereafter referred as “sr”) resulting from oil decantation were collected and separated by centrifugation at  $1520 \times g$  for 5 min (D3024 high-speed microcentrifuge, DLAB Scientific Inc., Riverside, CA, USA). Then, the pellets were washed four times with *n*-hexane to remove oil traces, and dried overnight. Attenuated Total Reflectance-Fourier Transform Infrared (ATR-FTIR) spectroscopy was applied to the powders, recording spectra in the wavenumber range  $4000\text{--}400\text{ cm}^{-1}$  by IRXross spectrophotometer (Shimadzu, Tokyo, Japan) with a resolution of  $4\text{ cm}^{-1}$  (45 scans). ATR-FTIR spectra were processed with Lab solution IR software (v.1.60, Shimadzu, Tokyo, Japan). Spectra were compared to those of the corresponding oil supernatants.

A preliminary UV-Vis investigation was also performed after solid/liquid extraction (yield of 1.2–1.5 %) by using a hydroalcoholic solution made of MeOH:H<sub>2</sub>O solution (4:1, v/v) in the ratio 1:10 w/v, and accelerated by ultrasounds (Ultrasonics™ Bransonic™ M3800-E; Danbury, CT, USA). UV-Vis spectra were recorded by the Cary 100 instrument (Agilent, Milano, Italy) in reference to a blank and compared to hydroalcoholic fractions (CO\_PhF and NCO\_PhF) obtained from HSO samples.

TPC in the solid residues resulting from oil decantation were determined using the same protocol above.

### 2.4. Statistical analysis

Statistical analysis was performed by using R software (R Core Team, 2022). Functional parameters of the press, y and PWR were analysed by one-way ANOVA with p value set at 0.05, with the use of the cooling mechanism as the main discriminant. The same approach was applied to determine if significative differences were obtained in the temperature markers in the thermograms, both between the 5 sampling sections (to assess the uniformity of the temperature during the extraction time) and between the NCO and CO thermograms to measure the detailed impact of the cooling system in any component of the screw press. Results from oil chemical analysis were compared using a two-way ANOVA based on the Tukey's multiple comparison test at a confidence level of 95 % ( $p < 0.05$ ), using the GraphPad Prism 8 software (Graphpad Software; La Jolla, CA, USA).

## 3. Results

### 3.1. Hemp seed oil cold pressing procedure

Chemical determinations showed that the extraction performances differed between the experimental traits. In particular, in the extraction chamber, the cooling system allowed the reduction of the T1 by 11 % on average, while the raw oil temperature (T2) was 15 % lower in the CO setup than in the NCO trials. The cooling system did not significantly influence the y in the oil extraction phase, since similar OGW and extraction times were obtained. Similarly, the PWR was not significantly affected by the different extraction conditions. Table 1

**Table 1**

Extraction results. Values are expressed as mean  $\pm$  SD. Different superscript letters indicate significant differences between treatments within the same parameter ( $p < 0.05$ , Tukey's post hoc test).

	T1 (°C)	OGW (g)	CGW (g)	T2 (°C)	y (% w/w)	PWR (Kg h <sup>-1</sup> )
CO	67.3 $\pm$ 0.5 <sup>a</sup>	222.5 $\pm$ 8.0	762.1 $\pm$ 9.5	22.5 $\pm$ 0.6 <sup>c</sup>	22.5 $\pm$ 0.0	13.7 $\pm$ 0.4
	75.6 $\pm$ 1.8 <sup>b</sup>	221.6 $\pm$ 4.1	754.8 $\pm$ 2.1	32.3 $\pm$ 0.7 <sup>d</sup>	22.2 $\pm$ 0.0	13.7 $\pm$ 0.6

The graphic outlook of the differences in the temperature is shown in Fig. 2. The photographs were snapped at a distance of 1.0 m setting an emissivity value of 1.5 temperature values were extrapolated from the pixels of the pictures (P1-P5 landmarks) to inspect the range of variations. At the same time the average temperature value, the Standard Deviation (SD), the minimum and the maximum in the whole area (AREA landmark) and across the horizontal profile of the screw chamber (LINE landmark) were reported in Table 2. Finally, in Fig. 3 the variations of temperature along the LINE landmark were compared.

All the temperature values reported in the landmarks from the NCO traits are higher compared to the same snaps in the CO trait. In both traits, the highest temperature levels correspond to the tightest section of the socket in the screw chamber (P5 landmark), where the pressure reaches the maximum level, and the hemp cake is exposed to the strongest extraction pressure. Significative differences were obtained for all the landmarks. In addition, in the “Line” and “Area” markers the 5 thermograms did not report significative differences between the sampling sections. Moreover, as reported in Table 2, the standard deviation values in the 5 sampling both in the “Line” and “Area” marker are sensibly higher in the NCO conditions than in the CO system.

While in the first half of the screw press, the temperatures keep the same range, as the seeds approach the section of the chamber where the nozzles are surrounded by the coil of the cooling system (right part of the graphic in Fig. 1). The results show that, in this section of the machine the hemp seeds are exposed to temperature 65–70 °C lower in the CO system than in the NCO trait, allowing to keep constantly the thermal level lower than 35 °C. The implications will be explained in the discussion section. The only region where the CO system reaches slightly higher values is in correspondence with the hopper of the screw press, where the surface of the coil is not covered by the cooling coils (as shown in the Fig. 1 in the Materials and Methods section).

### 3.2. Oil quality parameters

Free acidity of the cold-pressed HSO samples under investigation are reported in Fig. 4(a). Values are lower than the threshold recommended by the Codex Standard for edible fats and oils, which sets the maximum value at 2 %, clearly demonstrating the high quality of the seeds and of the extraction procedure, which did not induce hydrolytic rancidity of triacylglycerols. Moreover, no significant differences were detected by two-way ANOVA among CO and NCO, analysed at the time of extraction and after 140 days, indicating that this parameter was not affected under proper storage conditions (4 °C in the dark).

The peroxide value (PV) is a key indicator of lipid oxidation in fats and oils, reflecting the formation of primary oxidation products therein. Fig. 4(b) shows the results of PV trend during 140 days of storage for CO and NCO HSO samples. Both CO and NCO samples exhibited a comparable trend in peroxide value (PV), with a significant 2.2- to 2.3-fold increase ( $p < 0.0001$ ) after two months from opening. However, even after 140 days, the oxidative stability of both oils remained well below the recommended threshold of 15 mEq O<sub>2</sub>/kg for cold-pressed and virgin oils, with final PV values of 3.44 (NCO) and 2.79 (CO). The lower PV in CO samples further supports the protective effect of temperature control in mitigating lipid oxidation.

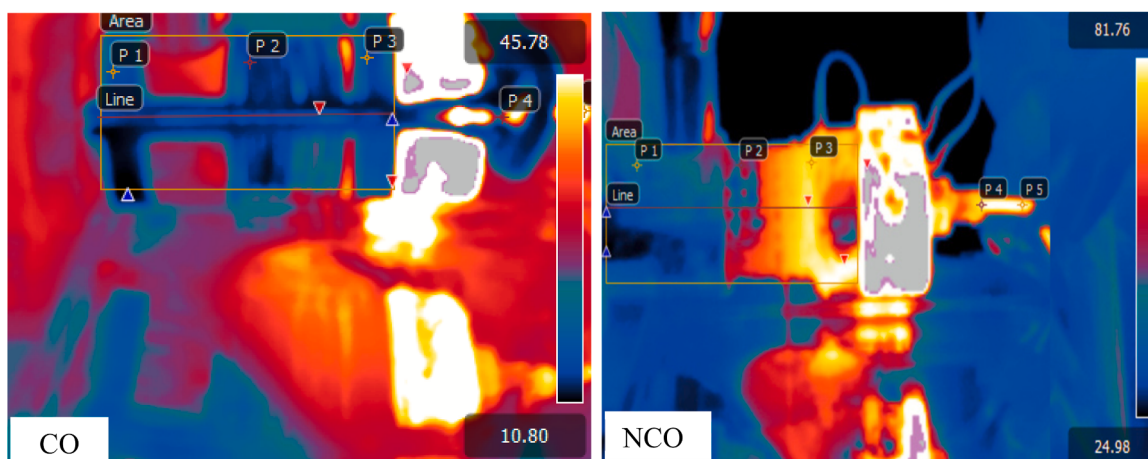


**Fig. 2.** Thermic photos snapped during the extraction of the hemp oil seed, with the landmarks position and the column bar of detected temperature ranges.

**Table 2**

Mean temperature values  $\pm$  SD in the selected landmarks (P1-P5, “Line”, “Area”) from the thermic images. Superscript letters (a–n) indicate statistically significant differences between CO and NCO within the same row ( $p < 0.05$ , Tukey's post hoc test).

Landmark	CO	NCO	P values
P1	$15.8 \pm 0.5^{\text{a}}$	$31.8 \pm 1.9^{\text{b}}$	7.6 E-08
P2	$15.0 \pm 1.9^{\text{c}}$	$50.9 \pm 6.0^{\text{d}}$	1.3 E-06
P3	$15.6 \pm 1.5^{\text{e}}$	$72.0 \pm 1.6^{\text{f}}$	9.6 E-12
P4	$34.3 \pm 4.2^{\text{g}}$	$69.8 \pm 4.9^{\text{h}}$	1.70E-06
P5	$54.4 \pm 6.8^{\text{i}}$	$73.3 \pm 5.8^{\text{j}}$	1.50E-03
Line	$15.5 \pm 1.4^{\text{k}}$	$45.1 \pm 16.0^{\text{l}}$	4.70E-08
Area	$19.9 \pm 5.2^{\text{m}}$	$44.5 \pm 12.5^{\text{n}}$	1.10E-08

To complement the quantification of PV, which is often paired with assessing secondary oxidation products contributing to oil rancidity, spectrophotometric parameters in the UV region were assessed, monitoring  $K_{232}$ ,  $K_{268}$ , and  $\Delta K$ , associated with the formation of peroxides and conjugated dienes (primary oxidation), conjugated trienes and peroxide decomposition to aldehydes and ketones (secondary oxidation). The results, reported in Fig. 4(c), showed higher values for NCO, which were 1.9-, 1.2-, and 1.4-fold for  $\Delta K$ ,  $K_{232}$ ,  $K_{268}$ , respectively. This evidence suggests that CO has a better quality from an oxidative point of view, underlining the positive impact of the cooling system during the extraction steps in delaying oxidation.

### 3.3. Free fatty acids and pre-cannabinoid profiling

CO and NCO samples, properly diluted in *n*-hexane, underwent a chemical profiling by UHPLC–HRMS to detect and quantify the main FFAs and verify the presence of pre-cannabinoids. As regards FFAs, although the official regulations suggest the GC determination after derivatization to the corresponding methyl esters, in our hands the use of UHPLC–MS tools proved to be effective in the detection of saturated and unsaturated medium- and long-chain FFAs following ionization in negative ion mode, both in HSO samples (Izzo et al., 2020), and in other plant matrices (Gravina et al., 2022; Pacifico et al., 2024).

Based on peak areas from XIC chromatograms, linoleic acid ( $m/z$  279.2319,  $C_{18}H_{32}O_2$ ,  $-3.9$  ppm mass error) was the most abundant, accounting for 40 and 41 % in CO and NCO samples, respectively. It was followed by  $\alpha$ -linolenic acid ( $m/z$  277.2169,  $C_{18}H_{30}O_2$ ,  $-1.4$  ppm mass error), which contributed to the total FFAs for 23 and 24 %, respectively. Taking into account also stearidonic acid ( $m/z$  275.2012,  $C_{18}H_{28}O_2$ ,  $-1.8$  ppm mass error) among  $\omega 3$  fatty acids, the  $\omega 6/\omega 3$  ratio was equal to 1.4 in both samples. The only detected monounsaturated acid was oleic acid ( $m/z$  281.2480,  $C_{18}H_{34}O_2$ ,  $-2.1$  ppm mass error), whereas the saturated stearic and palmitic acid were minor components. Fig 5

Similar considerations about the reliable use of LC–MS techniques could be applied to the pre-cannabinoid determination, as demonstrated in previous papers published by our research group (Piccolella et al., 2021; Nigro et al., 2022, 2020). Thus, a targeted analysis based on the  $m/z$  values of the main phytocannabinoids was performed. Fig. 6 depicts

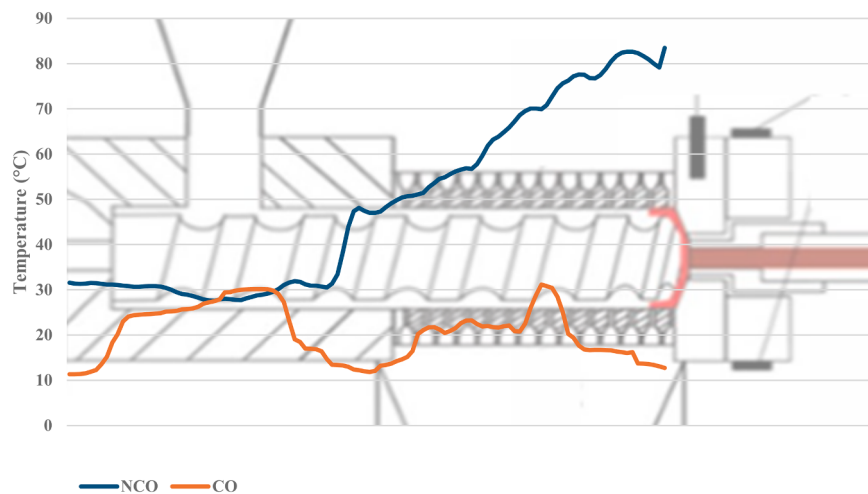


**Fig. 3.** Temperature variations in the NCO and the CO trait along the “Line” landmark during the hemp oil seed extraction phase.

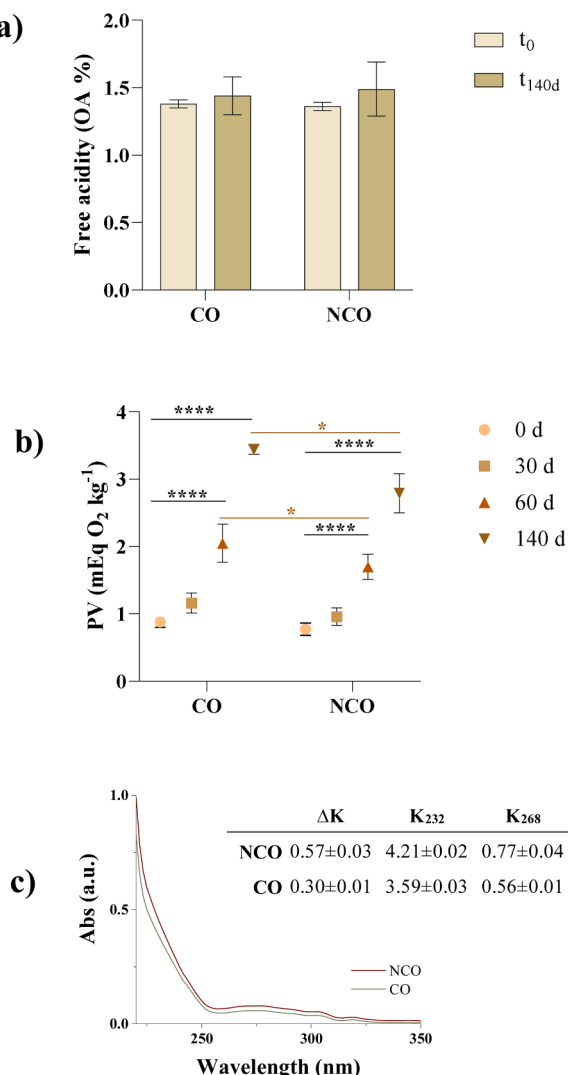


**Fig. 4.** a) Free acidity, expressed as oleic acid (OA) %, measured at  $t_0$  (immediately after cold-pressing and oil decantation) and  $t_{140d}$  (after 140 days storage) - p value > 0.5; b) Peroxide value, expressed as mEq O<sub>2</sub> kg<sup>-1</sup> oil, measured at four storage times (0, 30, 60, and 140 days). Cooling factor accounted for 91.33 % of the total variance. Only significant differences are highlighted (\*: p < 0.1; \*\*: p < 0.01; \*\*\*: p < 0.001; \*\*\*\*: p < 0.0001), calculated by GraphPad Prism 8 software (Graphpad Software. La Jolla. CA. USA). c) Spectrophotometric investigation in the UV region.

the Total Ion Current (TIC) chromatograms of CO and NCO samples, and the extracted ion chromatogram (XIC) for deprotonated CBDA at  $m/z$  357.2071 ± 0.01. The identity was confirmed comparing the Rt and the TOF-MS and TOF-MS/MS spectrum with data acquired for the CBDA previously purified and fully characterized (Formato et al., 2020). Moreover, following the characterization rules previously outlined (Piccolella et al., 2020, 2021), few traces of THCA-A and CBCA were detected (Rt 4.205 and 4.623 min, respectively). Their amount was below the limit of quantification.

On the contrary, based on the calibration curve built up using the pure compound, CBDA was quantified by HPLC-UV, exploiting the UV absorption band centered at 266 nm. The content of this pre-cannabinoid was similar in the two oil samples, being  $30.9 \pm 0.1$  and  $31.8 \pm 0.2$  mg kg<sup>-1</sup> oil in CO and NCO, respectively.

#### 3.4. Chlorophyll and carotenoid content

The content of the pigments in the investigated samples was

estimated spectrophotometrically, monitoring absorbance values in their peculiar range of light absorption. In Fig. 7, a representative UV-Vis spectrum is reported, together with the estimation of chlorophyll/carotenoid ratio. The results ( $2.786 \pm 0.19$  and  $2.750 \pm 0.40$  for CO and NCO, respectively), deriving from the calculated pigment amount expressed in ppm, did not show significant differences ascribable to the temperature in the extraction process.

#### 3.5. Tocopherol and total phenol content

Tocopherols, a group of fat-soluble antioxidants, play a crucial role in safeguarding HSO samples against oxidative degradation. Commonly found in plant-based oils, these compounds neutralize free radicals and inhibit the formation of peroxides and other oxidation products, thereby preserving oil stability. Herein, the content of tocopherols in CO and NCO samples was evaluated after cold saponification by HPLC-UV-DAD analysis, developing a fast and sensitive method able to detect the four vitamers with a good accuracy. The results were expressed as mg eq. of  $\alpha$ -tocopherol per kg of oil, based on the calibration curve of the commercial standard (Fig. 8). In line with previous reports and regardless the cooling system during extraction, HSO samples were particularly rich in  $\gamma$ -tocopherol ( $1015.4 \pm 122.7$  and  $972.3 \pm 78.9$  mg eq kg<sup>-1</sup>), with values slightly exceeding the maximum of the range reported in the current Regulation (UNI 11876:2022), likely due to a different detection mode. Moreover,  $\alpha$ -tocopherol ( $54.5 \pm 11.6$  and  $49.5 \pm 9.9$  mg eq kg<sup>-1</sup>),  $\delta$ -tocopherol ( $43.1 \pm 3.9$  and  $44.9 \pm 9.0$  mg eq kg<sup>-1</sup>) and  $\beta$ -tocopherol ( $27.6 \pm 6.5$  and  $24.1 \pm 3.6$  mg eq kg<sup>-1</sup>) were determined with a good accuracy.

In addition to tocopherols, HSO is known to contain variable amounts of phenols, classified as non-nutrient compounds, which have been associated with several potential health benefits. Indeed, they do not only contribute to plant tissue pigmentation but also serve as protective agents for the plant itself against exogenous stresses. After liquid/liquid fractionation, TPC was measured employing the Folin-Ciocalteu assay. It was found that their content in CO sample was slightly higher than that calculated for NCO ( $9.92 \pm 1.9$  vs  $6.18 \pm 1.6$  mg GAE g<sup>-1</sup> sample).

#### 3.6. Phytosterol content

The unsaponifiable fraction obtained after oil saponification was analysed by GC-FID. The identification was performed following a recent paper (Trovato et al., 2023), also regarding minor constituents. In Fig. 9(a) a representative chromatogram is depicted, whereas the content of each sterol is reported in Fig. 9(b), expressed as % of the total sterol content. As detected for tocopherols, also the phytosterol content was unaffected by temperature differences during the extraction, leading to almost superimposable amounts of these compounds in CO and NCO samples. As previously reported, the most representative constituent belonging to this class was  $\beta$ -sitosterol, accounting for  $65.34 \pm 1.0$  % and  $65.33 \pm 1.6$  % in CO and NCO, respectively, followed by campesterol ( $13.30 \pm 1.4$  % in both samples) and  $\Delta^5$ -avenasterol ( $6.96 \pm 0.2$  % and  $6.94 \pm 0.2$  %). All of them were in line with range values reported in the current Regulation (UNI 11876:2022). The estimated content for the other sterols was always below 5 %, although, if considered all together, their percentage could not be neglected.

#### 3.7. Spectroscopic characterization of the solid residues after oil decantation

Solid residues collected after oil decantation were washed with *n*-hexane to remove any oil traces, and after drying an extraction yield of  $5.78 \pm 0.01$  % w/v was estimated. The dried powders (CO\_sr and NCO\_sr) underwent ATR-FTIR analysis to record their molecular fingerprints based on vibrational absorptions of functional groups. Furthermore, data were compared to the corresponding CO and NCO samples. Spectra

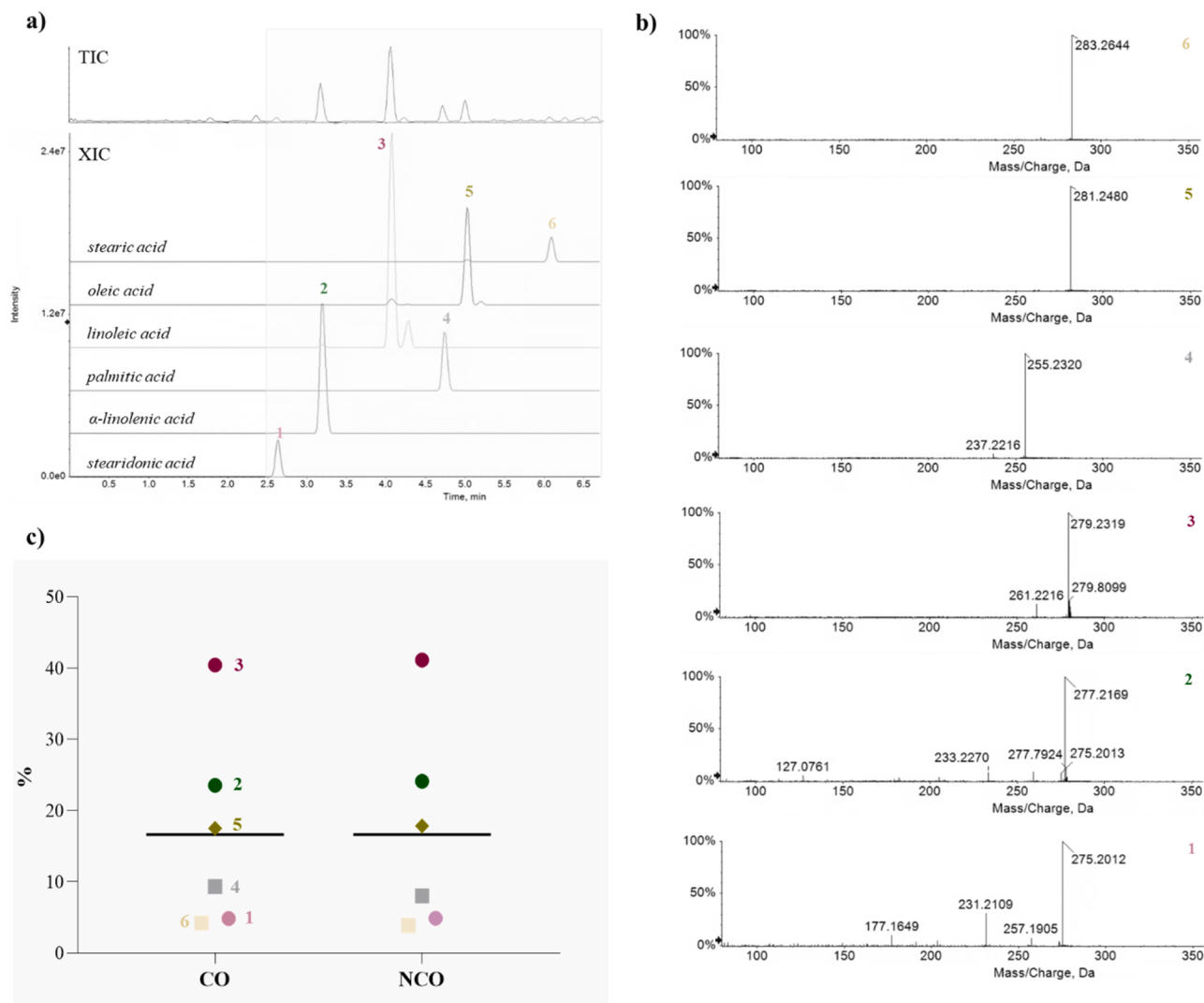


**Fig. 5.** a) Representative Total Ion Current (TIC) chromatogram, and the eXtracted Ion Chromatograms (XICs) for deprotonated free fatty acids, and b) their TOF-MS/MS spectra; c) relative quantitation (%) based on XIC peak areas.

obtained for these latter were superimposable (Fig. 10(a)), showing strong absorption bands in the C—H stretching region (2800–3000  $\text{cm}^{-1}$ ), due to the aliphatic methylene and methyl groups in fatty acid chains, supplemented by a weaker band at 3011  $\text{cm}^{-1}$  attributable to =C—H stretching of *cis*-double bonds in MUFA and PUFA constituents. Ester carbonyl (C=O) stretching vibrations of the triacylglycerol backbone were also detected at 1744  $\text{cm}^{-1}$ , confirming the glycerol fatty acid ester structure (Siano et al., 2019). Finally, multiple overlapping bending vibrations were detected in the fingerprint region (1500–600  $\text{cm}^{-1}$ ) based on data from the literature (Jović and Jović, 2017; Andronie et al., 2021), together with C—O stretching in COOR functional groups.

These signals massively decreased or even disappeared in the spectra recorded on the powdered residues (Figs. 10(b) and 10(c)), reasonably due to the removal of lipids by washing and centrifugation steps. Instead, new vibration modes were detected. Indeed, the typical N—H stretch of secondary amine was detected at 3280  $\text{cm}^{-1}$ , besides amide I due to C=O stretching vibrations and amide II of the C—N stretching vibrations in combination with N—H bending (at 1634  $\text{cm}^{-1}$  and 1541  $\text{cm}^{-1}$ , respectively) (Fig. 10(d)). This evidence, which is more noticeable in CO<sub>sr</sub>, could be related to the presence in the samples of phenyl-propanoid amides and their random oxidative coupling derivatives lignanamides, such as *N*-caffeoyletyramine or cannabinoids A and B, as

previously described (Nigro et al., 2020). Further confirmation of the presence of phenolic compounds derived from the UV-Vis spectroscopic analysis after hydroalcoholic extraction (Fig. 11), which allowed us to identify two main electronic transitions, associated with the  $\pi\rightarrow\pi^*$  transitions of aromatic moieties and  $n\rightarrow\pi^*$  and  $\pi\rightarrow\pi^*$  related to the amide group (Nigro et al., 2020).

The difference in the relative intensity suggested a different enrichment of the investigated samples. To corroborate this hypothesis, the Folin-Ciocalteu test was performed also on the extracted solid residues. As a general trend, the phenol content of the solid residues was up to 15-fold higher, compared to the oils. Being all seed-dependent parameters equal, the higher temperature in cold-pressing seems to favor the presence of phenols in the solid residue. In fact, contrary to the results obtained for oil samples, the TPC value calculated for NCO<sub>sr</sub> ( $95.65\pm7.8$  mg GAE g<sup>-1</sup> sample) was enhanced in comparison to that obtained for CO<sub>sr</sub> ( $77.69\pm11.1$  mg GAE g<sup>-1</sup> sample).

#### 4. Discussions

The optimization of extraction conditions aimed not only to maximize HSO yield but also to enhance sustainability in oil production, particularly through the careful control of rotation speed and temperature. The results confirm that the incorporation of a cooling system (CO)

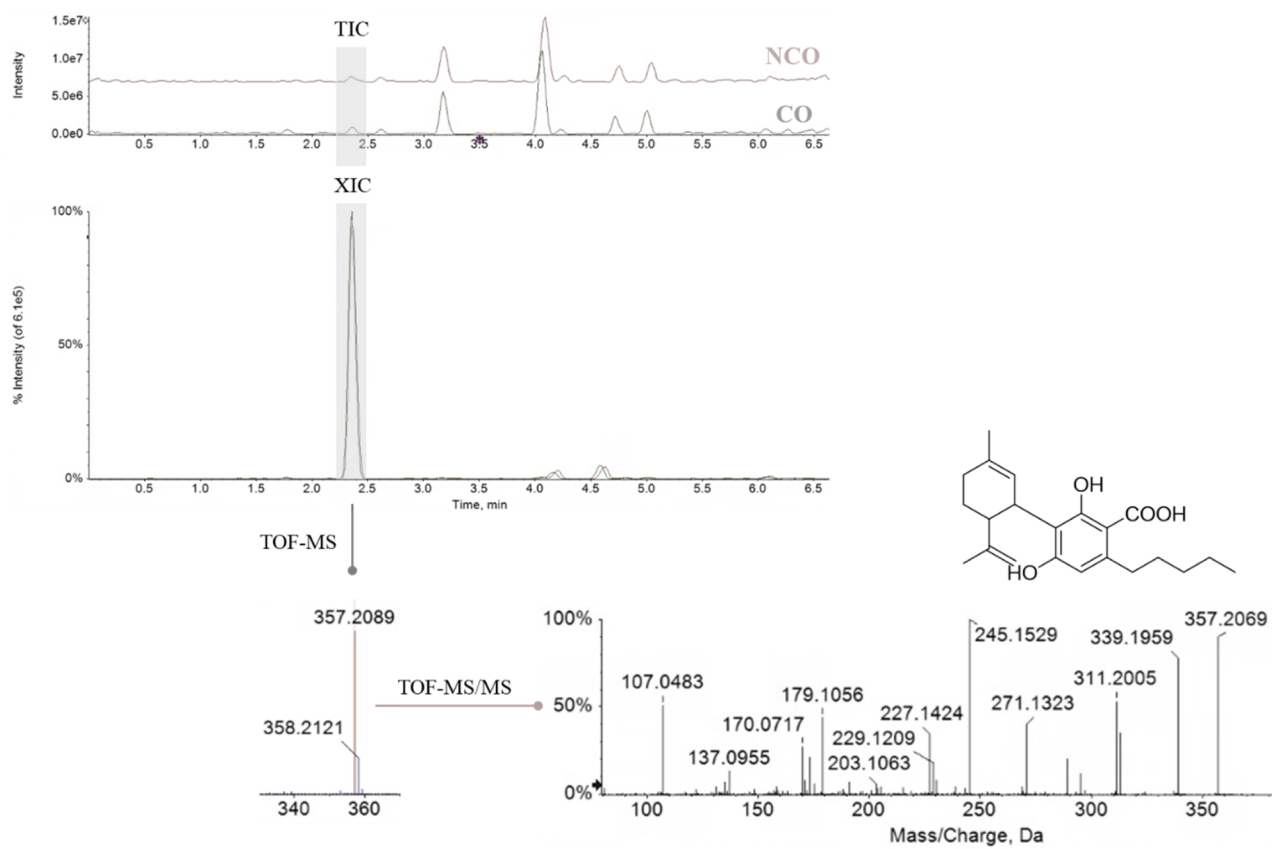


**Fig. 6.** Total Ion Current (TIC) chromatograms of CO and NCO samples, and the extracted ion chromatograms (XIC) for deprotonated CBDA at  $m/z$   $357.2071 \pm 0.01$ . Its structure, TOF-MS and TOF-MS/MS spectra are also depicted.

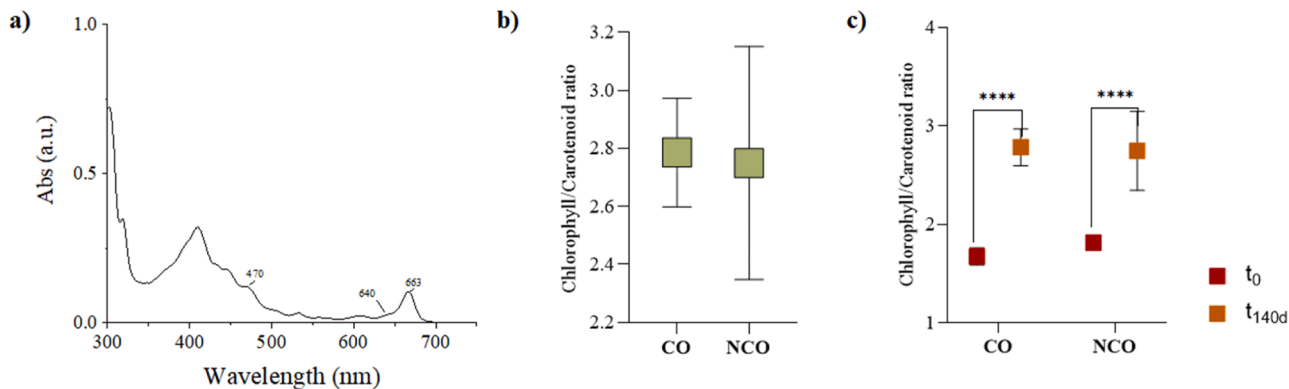


**Fig. 7.** a) Representative UV-Vis spectrum of hemp seed oils under study used for pigment determination; b) calculated ratio between chlorophylls and carotenoids after 140 days; c) two-way ANOVA comparison of pigments ratio based on cooling and time. This latter accounted for 85.13 % of total variation (\*\*\*\*:  $p < 0.0001$ ).

improved the extraction process without compromising operational efficiency, aligning with the need for energy-conscious and environmentally responsible production methods. The temperature ranges achieved in the CO system were consistent with the optimal extraction conditions reported in previous studies (Aladić, 2015), but with the additional advantage of significantly reducing the temperature of the extracted oil. This reduction is particularly relevant in a sustainable food system, as it helps minimize thermal degradation and the associated formation of oxidation byproducts, which can lead to waste and reduced product shelf life. By stabilizing temperature, the CO system contributes to the preservation of valuable volatile compounds, reducing the need for additional refining steps that are both resource-intensive and environmentally impactful. Previous studies (Sannino et al., 2024) have showed

that reducing nozzle diameter leads to higher oil yields. This finding is further supported by the results of the present investigation. A slight increase in yield was observed when the extraction temperature was lowered from 70 °C to 50 °C, using the same nozzle diameter and seed cultivar. Additionally, the pressing work rate (PWR) increased from 11.8 to 13.7 kg h<sup>-1</sup>, indicating that optimizing temperature control can improve productivity while reducing unnecessary energy expenditure. Given that low rotational speeds can expose oil to temperatures exceeding 70 °C, the heat reduction achieved through the CO system gains even more relevance, as it helps mitigate oxidation risks and extend the functional lifespan of the extracted oil, reducing losses throughout the production chain. Beyond processing conditions, agro-nomic factors such as harvesting time influence the lipid composition of

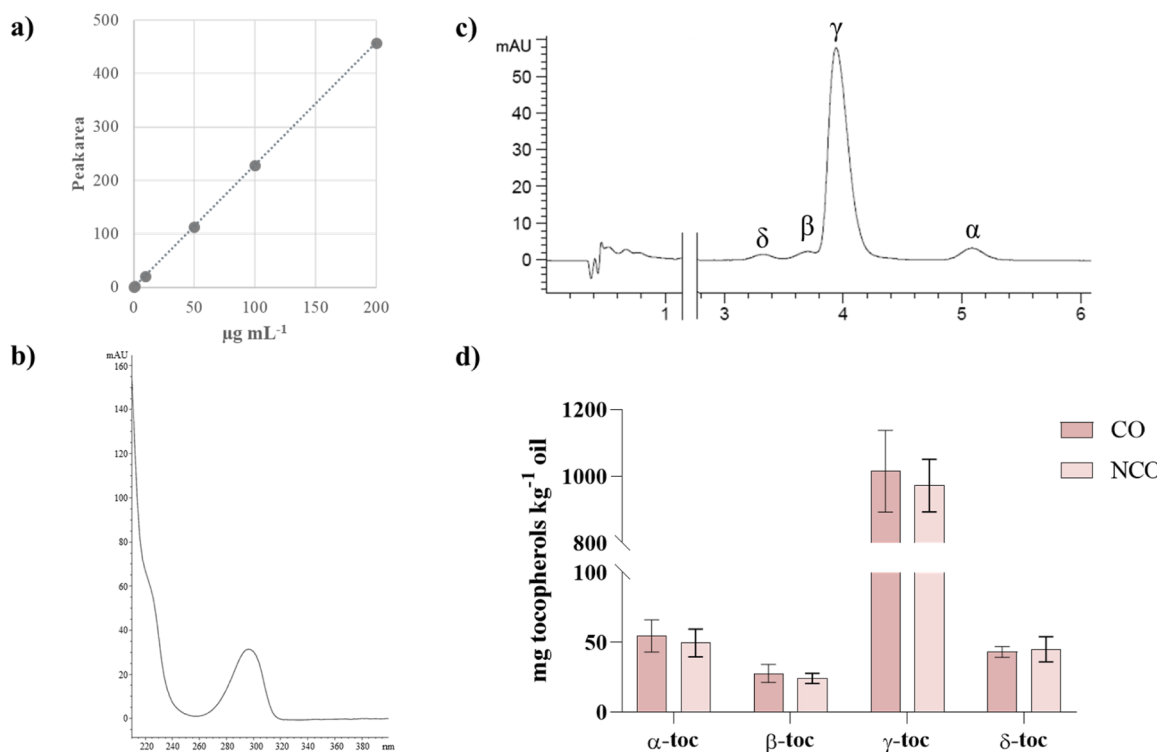


**Fig. 8.** a) Calibration curve of  $\alpha$ -tocopherol standard used for tocopherol quantitation; b) UV-DAD spectrum of  $\alpha$ -tocopherol standard; c) Representative HPLC-UV-DAD chromatogram of tocopherols detected in the investigated samples after cold saponification; d)  $\alpha$ -,  $\beta$ -,  $\gamma$ -, and  $\delta$ -tocopherol content expressed as  $\text{mg kg}^{-1}$  oil.

hemp seeds (Marzocchi and Caboni, 2020), ultimately affecting extraction efficiency. While not included in the scope of this study, their influence on oil yield is acknowledged, and further research should integrate agricultural and processing strategies to create a fully optimized, sustainable production model. At an industrial level, oilseed production efficiency is primarily assessed in terms of yield and operational capacity (Devi and Khanam, 2019). However, when considering long-term sustainability, it is also necessary to evaluate energy use, waste reduction, and the environmental impact of extraction methods. Techniques such as supercritical fluid extraction (SFE), while effective, require high pressures and solvents (Attard et al., 2018), increasing both energy demand and carbon footprint. In contrast, improving cold-pressing methods provides a lower-impact alternative, preserving nutrient-dense bioactive oils without excessive resource consumption.

The findings of this study suggest that the integration of a refrigerated screw press achieves an optimal balance between technical efficiency and environmental sustainability. Infrared thermographic analysis demonstrated that the CO system effectively stabilized extraction temperature, maintaining an upper limit of 67 °C, compared to peak temperatures exceeding 75 °C in the NCO system. This thermal stabilization played a critical role in preserving oil quality, as evidenced by lower peroxide values (PV) and reduced secondary oxidation markers (K232, K268,  $\Delta K$ ) in CO samples. By minimizing thermal stress, the CO system contributes to slower oxidative degradation, ensuring a longer-lasting and more stable end product. This temperature stabilization plays a crucial role in improving oxidative stability, as demonstrated by significantly lower peroxide values and secondary oxidation markers (K232, K268, and  $\Delta K$ ) in CO-extracted samples. From a sustainability perspective, this not only enhances oil quality but also reduces spoilage, lowers the need for preservatives, and minimizes product rejection, contributing to a more efficient use of raw materials.

Despite these quality and sustainability improvements, the cooling system did not negatively affect oil yield or pressing efficiency, confirming that high-quality extraction does not have to come at the expense of productivity (Table 3). Additionally, the tocopherol,

phytosterol, and fatty acid compositions remained stable, confirming that the cooling system effectively preserved the lipid fraction without causing alterations in its structural integrity. This highlights that the primary benefit of cooling lies in enhancing oxidative stability, rather than modifying the fundamental lipid profile. Maintaining this stability is crucial for ensuring the nutritional value and functional properties of the oil over extended storage periods. Interestingly, CO-extracted oils exhibited a significantly higher total phenolic content than NCO samples, highlighting the role of temperature control in preventing the degradation of antioxidant compounds. Given the established role of polyphenols in enhancing oxidative stability and providing health benefits, this increased retention directly contributes to the functional value of the oil. These findings emphasize that cooling-assisted cold pressing optimizes both oil stability and its bioactive potential, aligning with the rising demand for high-quality, functional plant-based oils.

The key differences observed between the CO and NCO systems are summarized in Table 3. The data reinforce the potential scalability of an integrated cooling system in industrial cold-pressing applications, offering a practical and energy-efficient solution to balance high extraction performance with sustainability goals. Given the increasing emphasis on eco-conscious food production, this study highlights the importance of optimizing mechanical extraction processes not only for higher yield and quality retention but also to ensure a lower environmental footprint in future large-scale applications. From an industrial perspective, the feasibility of integrating cooling systems into large-scale HSO production depends on multiple factors, including energy consumption, process efficiency, and environmental impact. While this study highlights significant advantages in oil quality and oxidative stability, large-scale implementation requires further assessment of cooling system performance and long-term sustainability.

A key challenge in scaling up is evaluating the energy trade-offs, as maintaining lower processing temperatures may increase power consumption. However, if properly optimized, the reduction in oxidative degradation and prolonged shelf life could contribute to lower resource waste and improve overall process sustainability. The integration of

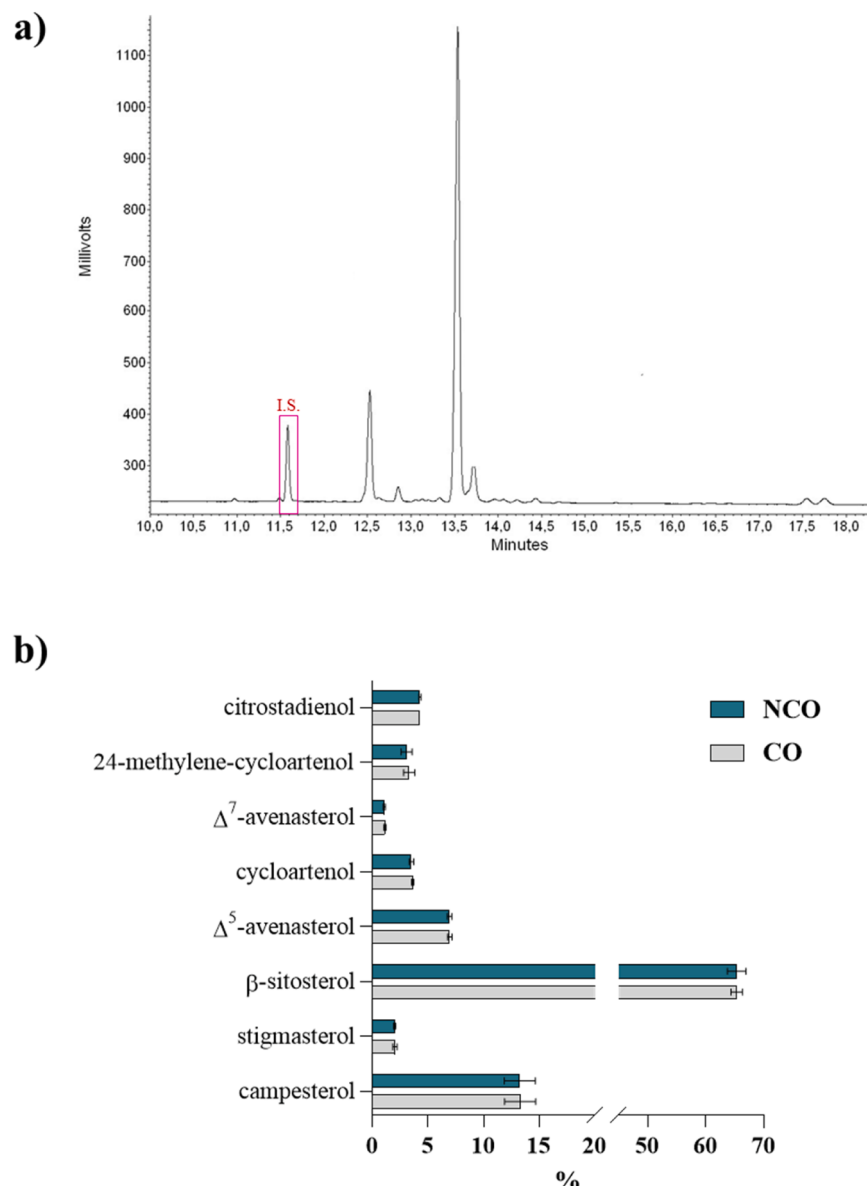


**Fig. 9.** a) Representative GC-FID chromatogram of hemp seed oil under study after saponification. IS = Internal Standard ( $\alpha$ -cholestane). b) Phytosterol content (expressed as % of the total sterol content) in CO and NCO samples.

energy-efficient cooling technologies, such as adaptive temperature regulation systems, could amplify these environmental benefits, aligning premium-quality HSO production with principles of low-impact and resource-conscious food manufacturing. The results underscore the technical feasibility of incorporating a refrigerated screw press system into larger-scale industrial operations. The consistency in oil yield and pressing rate, combined with improved oxidative stability, suggests that the CO system can be scaled without sacrificing productivity. While industrial adoption requires careful consideration of energy demands, advancements in energy-efficient cooling technologies, such as closed-loop systems, thermal insulation, and adaptive controls, offer viable solutions for minimizing added energy input. Moreover, the increased shelf life and reduced need for post-extraction refining could offset operational costs in the long term, making the process both economically and environmentally sustainable. Therefore, cooling-assisted pressing presents a scalable approach to meeting growing consumer demand for high-quality, clean-label plant-based oils.

## 5. Conclusions

Preserving the nutritional integrity of HSO is essential to fully exploit its health benefits. This requires understanding factors affecting the long-term stability of the oil after opening. One of the most crucial aspects is ensuring a high-quality seed supply, mainly with mature seeds having low moisture, optimized through careful selection of harvest timing and post-harvest management. Extraction temperature plays also a crucial role in maintaining the oil bioactive properties. In this context, integrating cooling systems into cold-pressing operations emerges as a viable and sustainable strategy to enhance HSO quality without compromising yield. Cold-pressed oil extraction is already a more sustainable alternative to conventional methods, avoiding solvents and excessive energy use. Cooling-assisted pressing mitigates thermal degradation, resulting in higher-quality oil with extended shelf life and improved nutritional value. These findings show that cooling-assisted cold pressing is a scalable and sustainable solution for industrial hemp seed oil production. The consistent oil yield and pressing efficiency confirm that the cooling-assisted system can be scaled up without

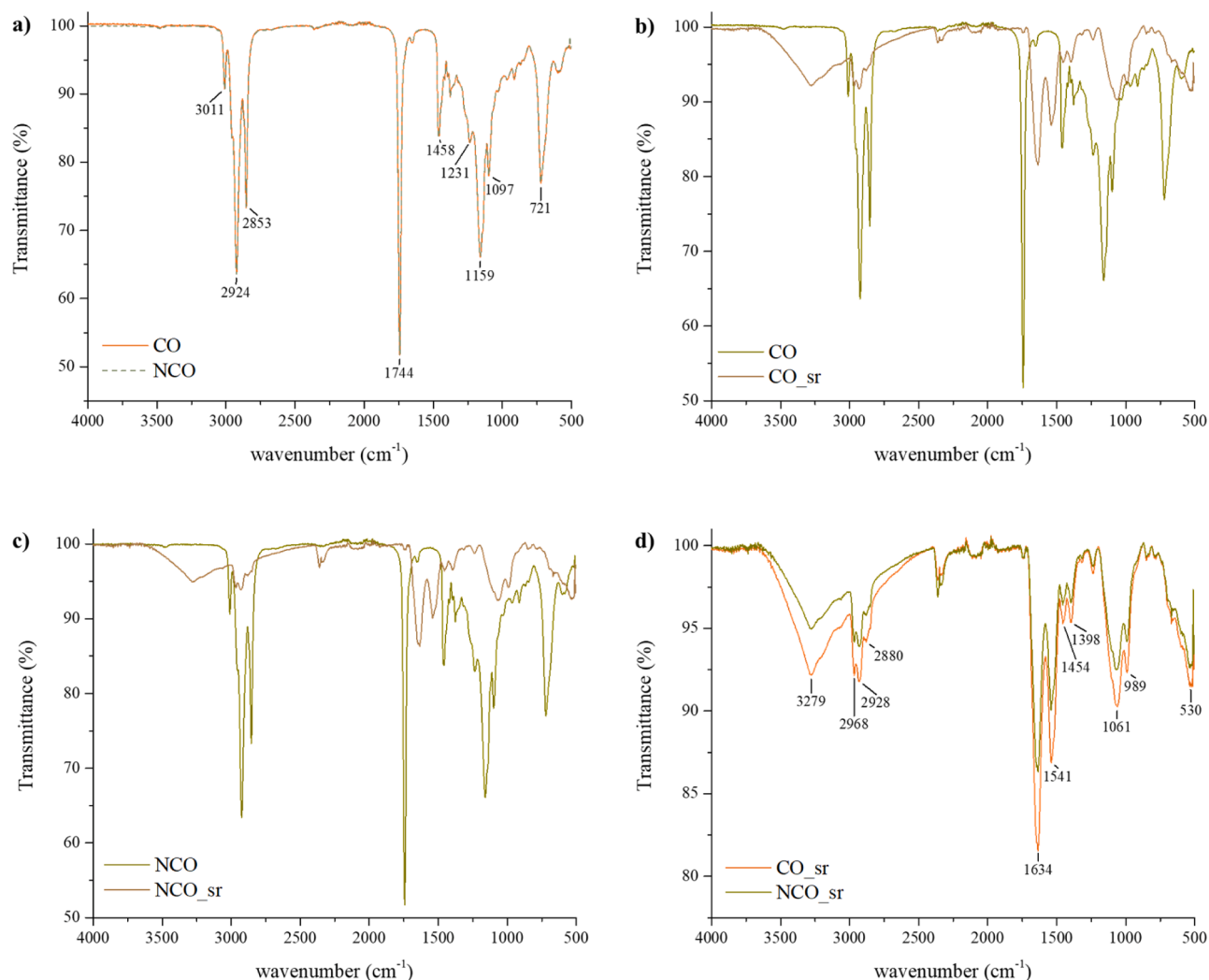


**Fig. 10.** ART FTIR of a) CO and NCO oil samples; b-c) CO and NCO spectra overlapped to the corresponding solid residue obtained through decantation; d) CO\_sr compared to NCO\_sr.

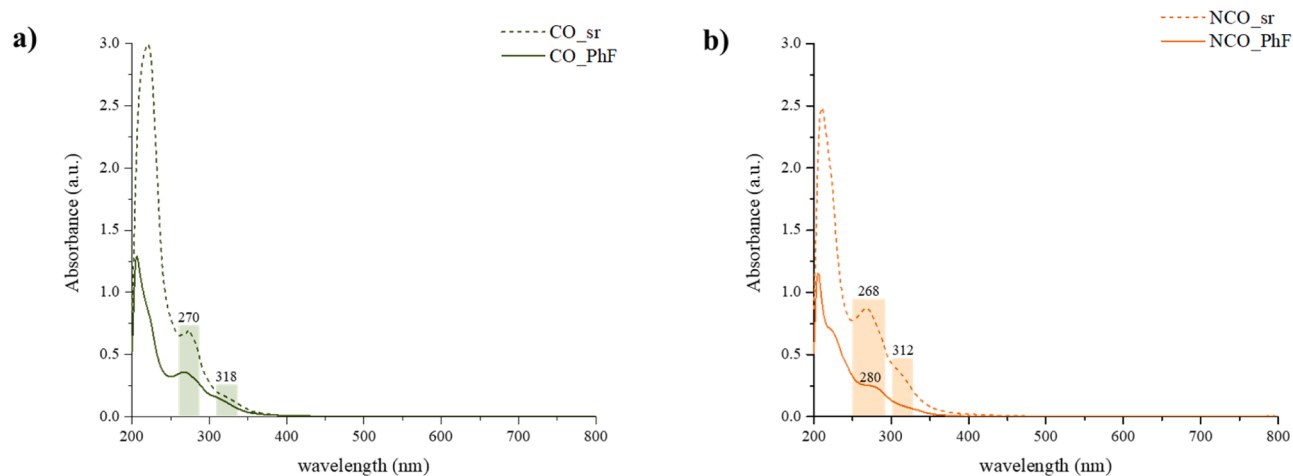


**Fig. 11.** UV-Vis spectra of phenolic fraction (PhF) extracted from hemp seed oils and from the solid residues (sr) after decantation of a) CO and b) NCO samples.

productivity loss, proving its industrial feasibility. This scalability allows commercial hemp seed oil production to benefit from improved quality and sustainability. Future research should optimize cooling parameters to enhance energy efficiency and oil stability, meeting growing demand

for eco-friendly, bioactive-rich plant oils. Sensory evaluations are also recommended to assess consumer acceptance and industrial applicability. Overall, the study successfully advances extraction methods that preserve nutritional quality and reduce environmental impact,

**Table 3**

Comparative overview of extraction conditions and oil quality parameters. CO = with cooling system; NCO = without cooling system; nsd = no significant difference.

Parameter	CO	NCO	Impact of Cooling System
Extraction Temperature (T1, °C)	67.3 ± 0.5	75.6 ± 1.8	↓ 11 % in chamber temperature
Extracted Oil Temperature (T2, °C)	22.5 ± 0.6	32.3 ± 0.7	↓ 15 % in oil temperature
Oil Yield (% w/w)	22.5 ± 0.0	22.2 ± 0.0	nsd
PV (mEq O <sub>2</sub> /kg oil, t140d)	2.79	3.44	lower oxidation in CO
ΔK (Secondary Oxidation Marker)	lower	higher	CO better prevents oxidation
TPC (mg GAE g <sup>-1</sup> oil)	9.92 ± 1.9	6.18 ± 1.6	higher retention in CO
Chlorophyll/Carotenoid Ratio	2.79 ± 0.19	2.75 ± 0.40	nsd
γ-tocopherol (mg/kg oil)	1015.4 ± 122.7	972.3 ± 78.9	slightly higher in CO
Phytosterol Content (% of total sterols, β-sitosterol)	65.34 ± 1.0	65.33 ± 1.6	nsd

supporting sustainable, high-value HSO production.

## Funding sources

This research did not receive any specific grant from funding agencies in the public, commercial, or not-for-profit sectors.

## Ethical statement - studies in humans and animals

This study did not involve human participants or animal subjects. Therefore, no ethical approval was required.

## CRediT authorship contribution statement

**Maura Sannino:** Investigation, Conceptualization, Writing – original draft, Data curation. **Simona Piccolella:** Investigation, Data curation, Writing – original draft, Formal analysis. **Guglielmo Maresca:** Formal analysis, Investigation. **Francesco Siano:** Investigation, Methodology. **Gianluca Picariello:** Investigation, Methodology. **Severina Pacifico:** Writing – original draft, Data curation, Writing – review & editing, Methodology. **Salvatore Faugno:** Supervision, Conceptualization, Visualization, Methodology.

## Declaration of competing interest

The authors declare that they have no known competing financial interests or personal relationships that could have appeared to influence the work reported in this paper.

## Acknowledgements

None.

## Data availability

Data will be made available on request.

## References

- AlMasoud, N., Munir, S., Alomar, T.S., Rabail, R., Hassan, S.A., Aadil, R.M., 2024. Impact of watermelon seed fortified crackers on hyperlipidemia in rats. *Pak Vet J* 44, 1291–1297. <https://doi.org/10.29261/pakvetj/2024.234>.
- Aladić, K., 2015. Cold pressing and supercritical CO<sub>2</sub> extraction of hemp (*Cannabis sativa*) seed oil. *Chemical and Biochemical Engineering Quarterly Journal* 28 (4), 481–490. <https://doi.org/10.1525/CABEQ.2013.1895>.
- Aloisi, I., Zoccali, M., Dugo, P., Tranchida, P.Q., Mondello, L., 2020. Fingerprinting of the unsaponifiable fraction of vegetable oils by using cryogenically-modulated comprehensive two-dimensional gas chromatography-high resolution time-of-flight mass spectrometry. *Food Anal Methods* 13, 1523–1529. <https://doi.org/10.1007/s12161-020-01773-9>.
- Andronie, L., Pop, I.D., Sobolu, R., Diaconeasa, Z., Trută, A., Hegeduş, C., Rotaru, A., 2021. Characterization of flax and hemp using spectrometric methods. *Applied Science* 11, 8341. <https://doi.org/10.3390/app11188341>.
- Attard, T.M., Bukhanko, N., Eriksson, D., Arshadi, M., Geladi, P., Bergsten, U., Budarin, V.L., Clark, J.H., Hunt, A.J., 2018. Supercritical extraction of waxes and lipids from biomass: a valuable first step towards an integrated biorefinery. *Journal of Cleaner Production* 177, 684–698. <https://doi.org/10.1016/j.jclepro.2017.12.155>.
- Calzolari, D., Rocchetti, G., Lucini, L., Amaducci, S., 2021. The variety, terroir, and harvest types affect the yield and the phenolic and sterolic profiles of hemp seed oil. *Food Research International* 142, 110212. <https://doi.org/10.1016/j.foodres.2021.110212>.
- CODEX STAN 210-1999 Codex Alimentarius, Standard for named vegetable oils, amended in 2005, 2011, 2013, 2015, 2019, 2021.
- COMMISSION REGULATION (EU) No 2023/915 of 25 April 2023 relating to maximum levels of certain contaminants in foods and repealing Regulation (EC) No. 1881/2006.
- Crescente, G., Piccolella, S., Esposito, A., Scognamiglio, M., Fiorentino, A., Pacifico, S., 2018. Chemical composition and nutraceutical properties of hempseed: an ancient food with actual functional value. *Phytochemistry Reviews* 17, 733–749. <https://doi.org/10.1007/s11101-018-9556-2>.
- Crimaldi, M., Faugno, S., Sannino, M., Ardito, L., 2017. Optimization of hemp seeds (*Cannabis sativa* L.) oil mechanical extraction. *Chemical Engineering Transactions* 58, 373–378. <https://doi.org/10.3303/CET1758063>.
- Devi, V., Khanam, S., 2019. Comparative study of different extraction processes for hemp (*Cannabis sativa*) seed oil considering physical, chemical and industrial-scale economic aspects. *Journal of Cleaner Production* 207, 645–657. <https://doi.org/10.1016/j.jclepro.2018.10.036>.
- Faugno, S., Piccolella, S., Sannino, M., Principio, L., Crescente, G., Baldi, G.M., Fiorentino, N., Pacifico, S., 2019. Can agronomic practices and cold-pressing extraction parameters affect phenols and polyphenols content in hempseed oils? *Industrial Crops and Products* 130, 511–519. <https://doi.org/10.1016/j.indcrop.2018.12.084>.
- Formato, M., Cresente, G., Scognamiglio, M., Fiorentino, A., Pecoraro, M.T., Piccolella, S., Catauro, M., Pacifico, S., 2020. (-)-Cannabidiolic acid, a still overlooked bioactive compound: an introductory review and preliminary research. *Molecules* 25, 2638. <https://doi.org/10.3390/molecules25112638>.
- Gravina, C., Fiorentino, M., Formato, M., Pecoraro, M.T., Piccolella, S., Stinca, A., Pacifico, S., Esposito, A., 2022. LC-HR/MS analysis of lipophilic extracts from *calendula arvensis* (Vaill.) L. Organs: an unexplored source in cosmeceuticals. *Molecules* 27, 8905. <https://doi.org/10.3390/molecules27248905>.
- Hafeez, H., Israr, B., Butt, M.S., Faisal, M.N., 2024. Therapeutic intervention of *Opuntia Ficus Indica* (L.) fruit and seed powder against CCl<sub>4</sub>-induced acute liver injury in wistar rats. *Pakistan Veterinary Journal* 44, 369–376. <https://doi.org/10.29261/pakvetj/2024.158>.
- Ionescu, M., Voicu, G., Sorin-Stefan, B., Covaliu, C., Dincă, M., Ungureanu, N., 2014. Parameters influencing the screw pressing process of oilseed materials. 3rd International Conference on Thermal Equipment, Renewable Energy and Rural Development. TE-RE-RD 243–248.
- Izzo, L., Pacifico, S., Piccolella, S., Castaldo, L., Narváez, A., Grosso, M., Ritieni, A., 2020. Chemical analysis of minor bioactive components and cannabidiolic acid in commercial hemp seed oil. *Molecules* 25 (16), 3710. <https://doi.org/10.3390/molecules25163710>.
- Jović, H., Jović, A., 2017. FTIR-ATR adulteration study of hempseed oil of different geographic origins. *Journal of Chemometrics*. <https://doi.org/10.1002/cem.2938> e2938.
- Karaj, S., Müller, J., 2011. Optimizing mechanical oil extraction of *Jatropha curcas* L. seeds with respect to press capacity, oil recovery and energy efficiency. *Industrial Crops and Products* 34 (1), 1010–1016. <https://doi.org/10.1016/j.indcrop.2011.03.009>.
- Kraljić, K., Škevin, D., Pospišil, M., Obračanović, M., Neđjerić, S., Bosolt, T., 2013. Quality of rapeseed oil produced by conditioning seeds at modest temperatures. *Journal of the American Oil Chemists' Society* 90 (4), 589–599. <https://doi.org/10.1007/s11746-012-2195-7>.
- Tura, M., Mandrioli, M., Valli, E., Gallina Toschi, T., 2023. Quality indexes and composition of 13 commercial hemp seed oils. *Journal of Food Composition and Analysis* 117, 105112. <https://doi.org/10.1016/j.jfca.2022.105112>.
- Marzocchi, S., Caboni, M., 2020. Effect of harvesting time on hemp (*Cannabis sativa* L.) seed oil lipid composition. *Italian Journal of Food Science* 32 (4). <https://doi.org/10.14674/IJFS.1898>.
- Mistry, M., Turumella, S., Prajapati, V., Dholakiya, B.Z., 2025. Harnessing hemp seed oil for a circular bioeconomy: a data-driven exploration of sustainable applications for next-generation industries. *Bioresource Technology Report* 30, 102126. <https://doi.org/10.1016/j.briteb.2025.102126>.
- Montero, L., Ballesteros-Vivas, D., Gonzalez-Barrios, A.F., Sánchez-Camargo, A.D.P., 2023. Hemp seeds: nutritional value, associated bioactivities and the potential food applications in the Colombian context. *Frontiers in Nutrition* 9, 1039180. <https://doi.org/10.3389/fnut.2022.1039180>.

- Muangrat, R., Kaikonjanat, A., 2025. Comparative evaluation of hemp seed oil yield and physicochemical properties using supercritical CO<sub>2</sub>, accelerated hexane, and screw press extraction techniques. *Journal of Agriculture and Food Research* 19, 101618. <https://doi.org/10.1016/j.jafr.2024.101618>.
- Nigro, E., Crescente, G., Formato, M., Pecoraro, M.T., Mallardo, M., Piccolella, S., Daniele, A., Pacifico, S., 2020. Hempseed lignanamides rich-fraction: chemical investigation and cytotoxicity towards U-87 glioblastoma cells. *Molecules* 25, 1049. <https://doi.org/10.3390/molecules25051049>.
- Nigro, E., Pecoraro, M.T., Formato, M., Piccolella, S., Ragucci, S., Mallardo, M., Russo, R., Di Maro, A., Daniele, A., Pacifico, S., 2022. Cannabidiolic acid in hemp seed oil table spoon and beyond. *Molecules* 27, 2566. <https://doi.org/10.3390/molecules27082566>.
- Pacifico, S., Caputo, E., Piccolella, S., Mandrich, L., 2024. Exploring new fruit- and vegetable-derived rennet for cheese making. *Applied Sciences* 14, 2257. <https://doi.org/10.3390/app14062257>.
- Piccolella, S., Crescente, G., Formato, M., Pacifico, S., 2020. A cup of hemp coffee by Moka Pot from Southern Italy: an UHPLC-HRMS investigation. *Foods* 9, 1123. <https://doi.org/10.3390/foods9081123>.
- Piccolella, S., Formato, M., Pecoraro, M.T., Crescente, G., Pacifico, S., 2021. Discrimination of CBD-, THC- and CBC-type acid cannabinoids through diagnostic ions by UHPLC-HR-MS/MS in negative ion mode. *Journal of Pharmaceutical and Biomedical Analysis* 201, 114125. <https://doi.org/10.1016/j.jpba.2021.114125>.
- Piravi-Vanak, Z., Dadazadeh, A., Azadmard-Damirchi, S., Torbati, M., Martinez, F., 2024. The effect of extraction by pressing at different temperatures on sesame oil quality characteristics. *Foods* 13, 1472. <https://doi.org/10.3390/foods13101472>.
- R Core Team, 2022. R: A Language and Environment for Statistical Computing. R Foundation for Statistical Computing. <https://www.r-project.org/>.
- Saleh, M., Ramadan, M., Elmadawy, R., Morsi, M., El-Akabawy, L., 2023. The efficacy of alcoholic extracts of *Morus macroura* (mulberries), *Lepidium sativum* (garden cress seeds) and diclazuril against *E. stiedae* in experimentally infected rabbits. *International Journal of Veterinary Science* 12, 869–878. <https://doi.org/10.47278/journal.ijvs/2023.049>.
- Sannino, M., Vastolo, A., Faugno, S., Masucci, F., Di Francia, A., Sarubbi, F., Pelosi, M.E., Kiatto, D.D., Serrapica, F., 2024. The use of small diameter nozzles in temperature-controlled hemp oil extraction allows high oil yields and good quality residual hemp cake feed. *Frontiers in Veterinary Science* 10, 1322637. <https://doi.org/10.3389/fvets.2023.1322637>.
- Senphan, T., Mungmueang, N., Srikit, C., Srikit, P., Sinthusamran, S., Narkthewan, P., 2025. Influence of extraction methods and temperature on hemp seed oil stability: a comprehensive quality assessment. *Applied Food Research* 5, 100702. <https://doi.org/10.1016/j.afres.2025.100702>.
- Siano, F., Moccia, S., Picariello, G., Russo, G.L., Sorrentino, G., Di Stasio, M., La Cara, F., Volpe, M.G., 2019. Comparative study of chemical, biochemical characteristic and ATR-FTIR analysis of seeds, oil and flour of the edible fedora cultivar hemp (*Cannabis sativa* L.). *Molecules* 24, 83. <https://doi.org/10.3390/molecules24010083>.
- Trovato, E., Arena, K., La Tella, R., Rigano, F., Laganà Vinci, R., Dugo, P., Mondello, L., Guarnaccia, P., 2023. Hemp seed-based food products as functional foods: a comprehensive characterization of secondary metabolites using liquid and gas chromatography methods. *Journal of Food Composition and Analysis* 117, 105151. <https://doi.org/10.1016/j.jfca.2023.105151>.
- UNI 11876:2022, 2022. Vegetable and animal oils and fats and derivatives – Cold-pressed hemp oil, obtained from the seeds of *Cannabis sativa* L. Characteristics and Methods of Analysis.

## Further readings

- Kabutey, A., Herák, D., Mizera, Č., 2023. Assessment of quality and efficiency of cold-pressed oil from selected oilseeds. *Foods* 12 (19), 3636. <https://doi.org/10.3390/foods12193636>.
- Rahman, A., Cho, B.-K., 2016. Assessment of seed quality using non-destructive measurement techniques: a review. *Seed Science Research* 26 (4), 285–305. <https://doi.org/10.1017/S0960258516000234>.
- ISO 9936:2016, 2016. Animal and vegetable fats and oils — Determination of tocopherol and tocotrienol contents by high-performance liquid chromatography. International Organization for Standardization.